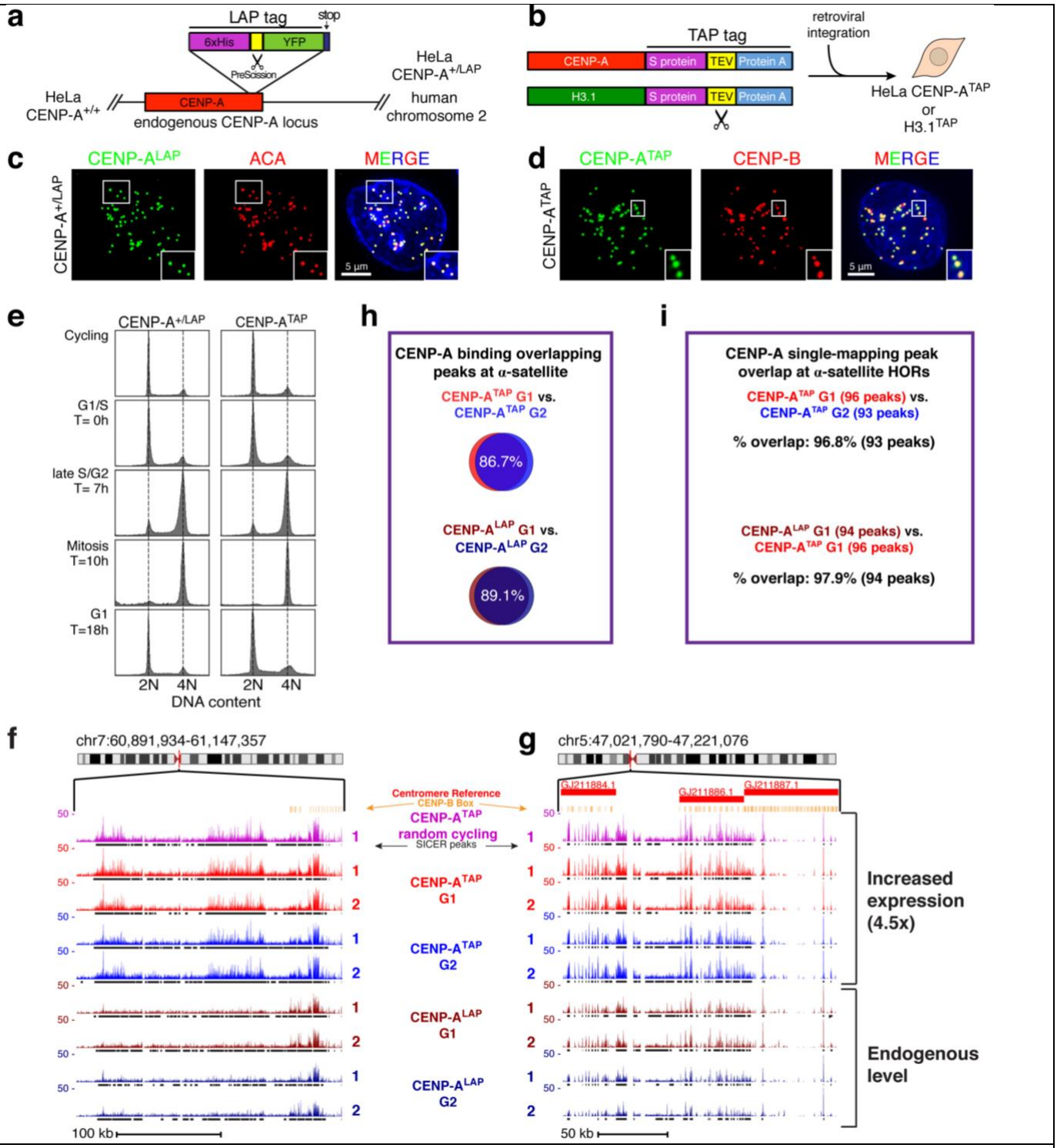

Supplementary Figure 1

Identification of peaks enriched for CENP-A binding.

(a) Scheme showing experimental design for tagging an endogenous CENP-A locus to produce CENP-A+/LAP HeLa cells. These cells were then adapted to suspension growth. (**b**) Scheme showing the experimental design for obtaining increased levels of CENP-ATAP expression. CENP-ATAP is expressed in these cells at 4.5-fold the level of CENP-A in the parental HeLa cells1. **(c, d)** Localization of

endogenously tagged CENP-A$_{LAP}$ (c) and CENP-A$_{TAP}$ (d) determined with indirect immunofluorescence using anti-GFP antibody (c) or rabbit-IgG (d). Scale bar, 5 μm. The experiment was repeated independently three times with similar results for both (c) and (d). (**e**) FACS analysis of DNA content showing the synchronization efficiency of CENP-A$_{+/LAP}$ and CENP-A$_{TAP}$ HeLa cell lines. The experiment was repeated independently five times with similar results. (**f**, **g**) Examples of centromeric regions of chromosome 7 (f) and 5 (g) showing increased occupancy of overexpressed CENP-A$_{TAP}$ (compare CENP-A$_{TAP}$ with CENP-A$_{LAP}$). The experiment was repeated independently twice with similar results**.** (**h**) Overlap between G1 and G2 CENP-A binding peaks at α-satellite sequences. (**i**) Top, overlap between G1 and G2 CENP-A single mapping binding sites at α-satellite HOR sequences. Bottom, peak overlap between G1 CENP-A$_{TAP}$ (increased expression) and CENP-A$_{LAP}$ (endogenous level) single mapping binding sites at α-satellite HOR sequences.

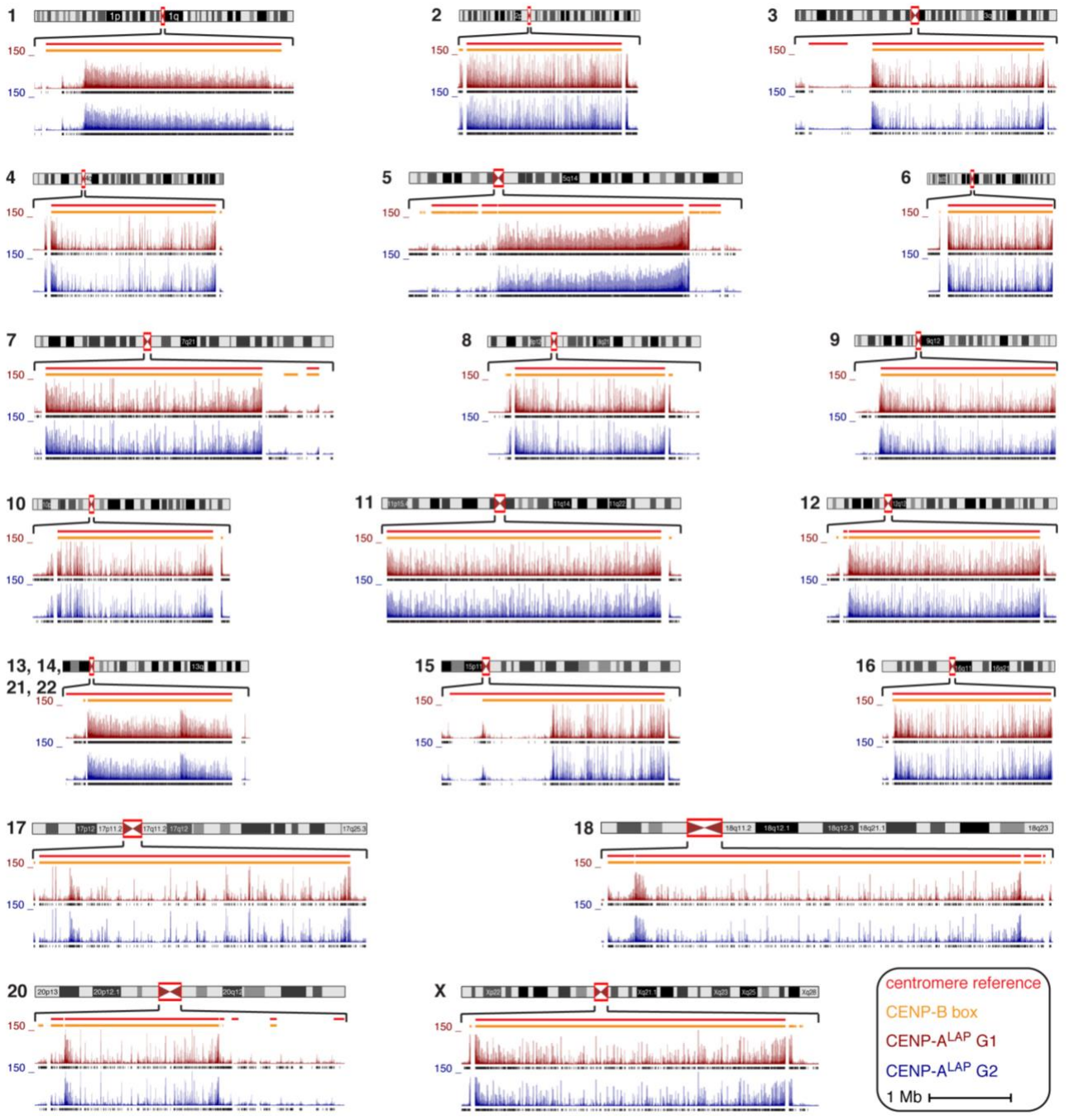

Supplementary Figure 2

CENP-A ChIP-seq identifies CENP-A binding at reference centromeres of 23 human chromosomes.

CENP-A$_{LAP}$ bound DNAs at G1 and G2 were sequenced, with 2 replicates per condition, and mapped to the centromeric reference models in the hg38 assembly[2, 3]. Shown are the raw mapping data (colored) for every human centromere (except for the centromere of chromosome 19 that shares almost all of its α-satellites arrays with α-satellites arrays of chromosomes 1 and 5) and CENP-A binding called as SICER peaks (black lines, underneath) for one replicate for each time point. The experiment was repeated twice independently with similar results. Centromere reference location, red. CENP-B box, orange.

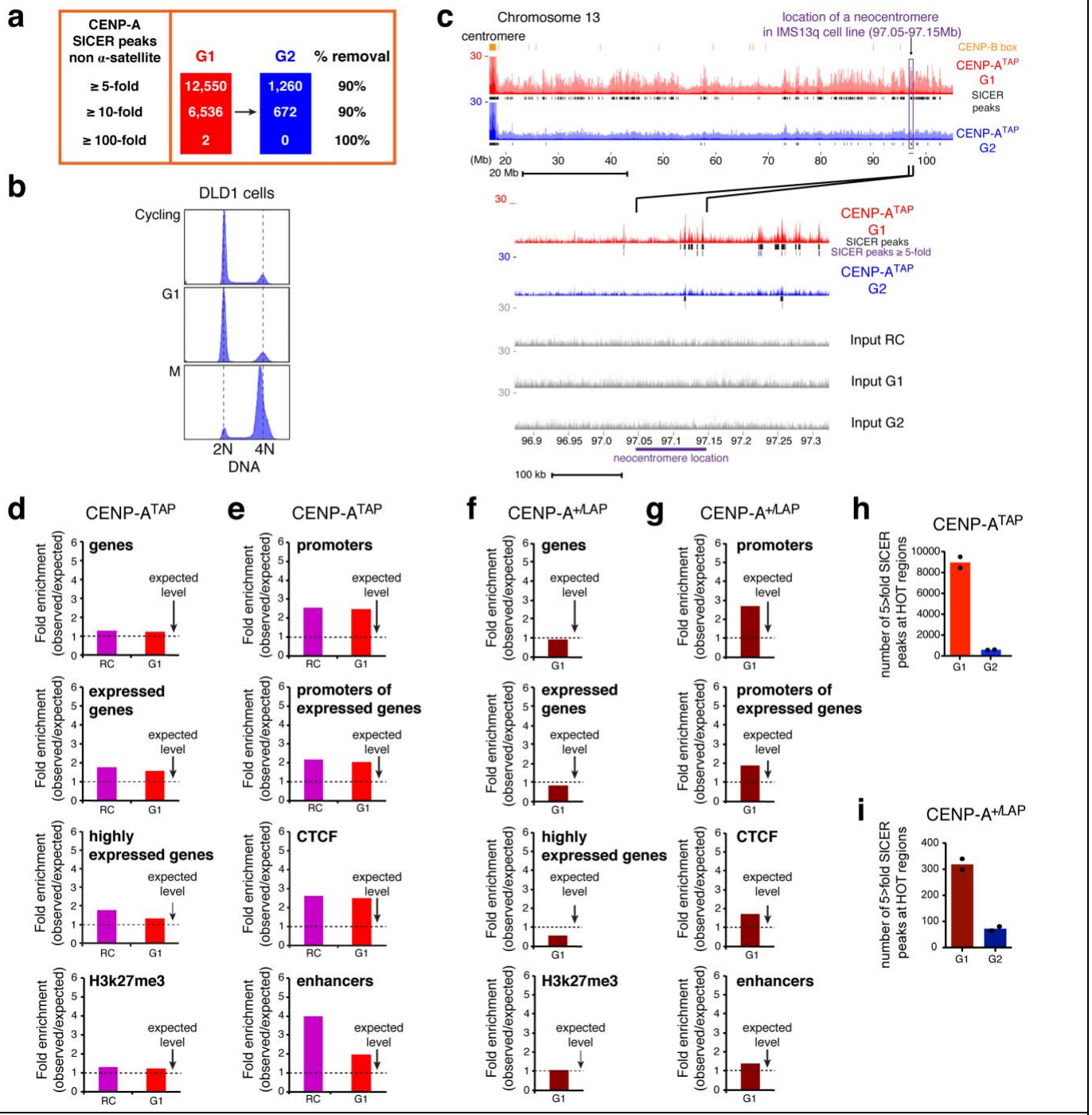

Supplementary Figure 3

Ectopic deposition of CENP-A into open and active chromatin at G1 does not function as a seeding hotspot for neocentromere formation.

(**a**) Number of non-α-satellite CENP-A SICER binding sites called at G1 or G2 at different fold thresholds (above background). (**b**) Human DLD1 cells with auxin degradable CENP-A^{AID} and a doxycycline-inducible CENP-A$^{WT\ 4}$, were synchronized at G1 using the CDK4/6 inhibitor PD-0332991 (also known as Palbociclib) or at mitosis using nocodazole, following addition of doxycycline. The experiment was repeated independently three times with similar results. (**c**) Read mapping data of CENP-A^{TAP} ChIP-sequencing at G1 (red) and G2

(blue), at the chromosomal location of a known patient derived neocentromere[5] found in chromosome 13. The experiment was repeated twice independently with similar results. A third human neocentromere, identified in line MS4221, has been identified to lie within a 400 kb neocentromere at position 86.5 to 86.9 Mb on chromosome 8 in hg19[5, 6] (corresponding to 85.78-85.88 Mb in hg38). However, a gap and segmental duplications that appear in this region precluded precise analysis of CENP-A mapping at this neocentromere. **(d-g**) Fold enrichment of CENP-A$_{TAP}$ chromatin in randomly cycling cells or at G1 (**d, e**) and CENP-A$_{LAP}$ chromatin (**f, g**) at G1 at different genomic locations. SICER peaks ≥ 5-fold supported between two replicates were analyzed for their enrichment level at different genomic locations, compared to the level of enrichment at these sites by chance. (**h, i**) Number of CENP-A$_{TAP}$ (h) and CENP-A$_{LAP}$ (i) SICER peaks ≥ 5-fold that overlap with 'HOT' regions in the human genome in G1 and G2 synchronized cells. Data shown are from two biologically independent experiments. Source data for d-i can be found in Supplementary Table 4.

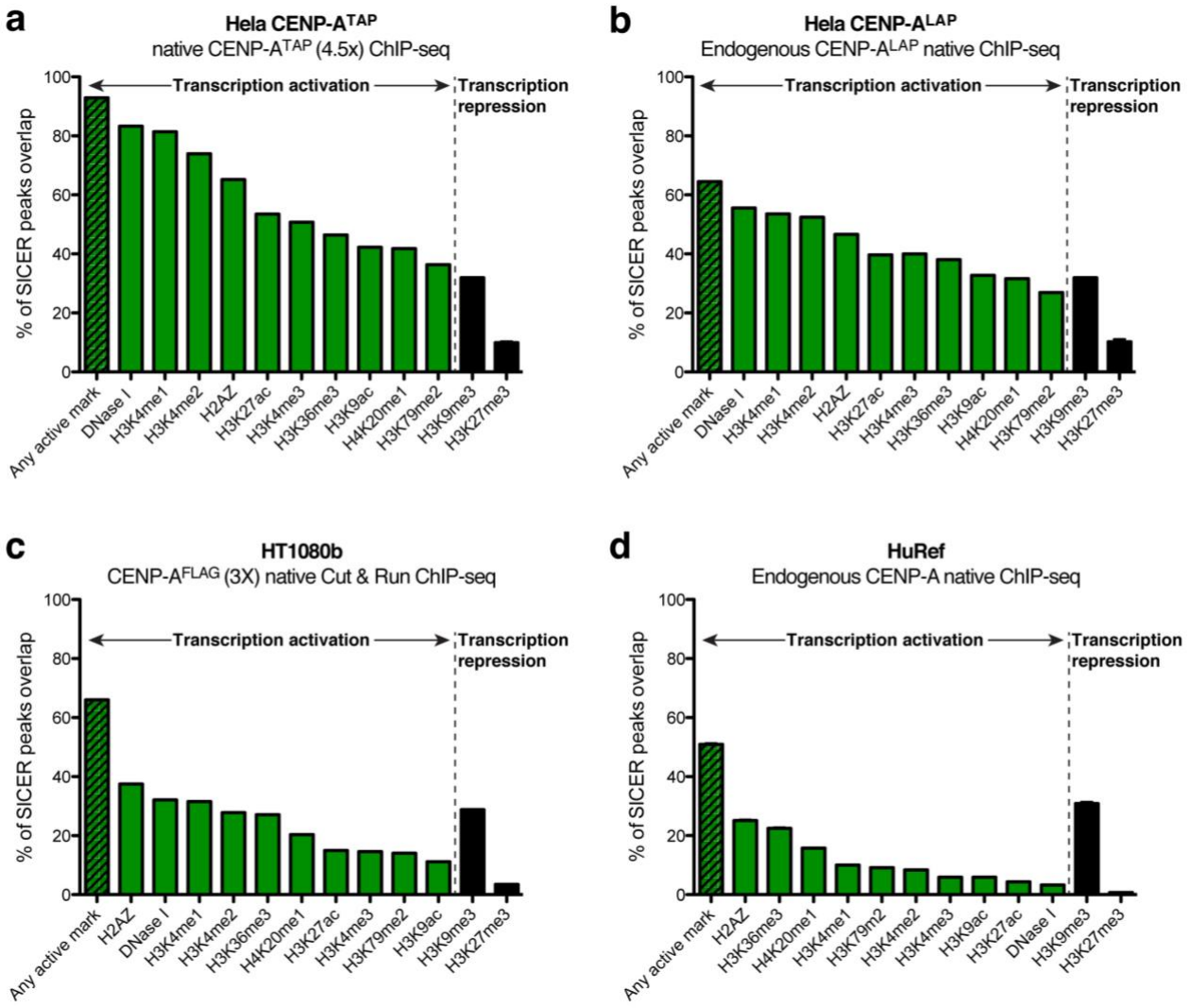

Supplementary Figure 4

Non-centromeric CENP-A binding peaks overlap with active transcription marks.

(**a,b**) The chromatin features of CENP-A$_{TAP}$ (a) and CENP-A$_{LAP}$ (b) non-centromeric preferential sites were analyzed by intersecting SICER peaks ≥ 5-fold supported between two replicates with publicly available ENCODE datasets for histone modification profiles in HeLa-S3, that represent modifications typically associated with transcription activation or repression. The experiment was performed one time, except for DNase I and H3K27me3 for which there are 2 ENCODE datasets available, and therefore for DNase I and H3K27me3 the experiment was repeated twice independently with similar results. Statistics source data for Supplementary Fig 4a,b can be found in Supplementary Table 4. (The sum of ectopic CENP-A$_{TAP}$ sites at active or repression marks is more than 100%, the result of overlap between H3K9me3 and active transcription marks.) (**c,d**) The chromatin features of sites of preferential, non-centromeric CENP-A binding were analyzed for histone modification profiles associated with transcription activation or repression in HeLa-S3 cells by intersecting SICER peaks ≥ 5-fold found in previously published CENP-A ChIP-seq datasets in HT1080[7] (c) and HuRef[8] (d) cell lines with publicly available ENCODE datasets for histone modification profiles in HeLa-S3. For HT1080b (c) the experiment was performed one time, except for DNase I and H3K27me3 for which there are 2 ENCODE datasets available, and therefore for DNase I and H3K27me3 the experiment was repeated twice independently with similar results. For HuRef (d), The experiment was performed four times, except for DNase I and H3K27me3 for which there are 2 ENCODE datasets available, and therefore for DNase I and H3K27me3 the experiment was repeated independently eight times with similar results. Source data for a-d can be found in Supplementary Table 4.

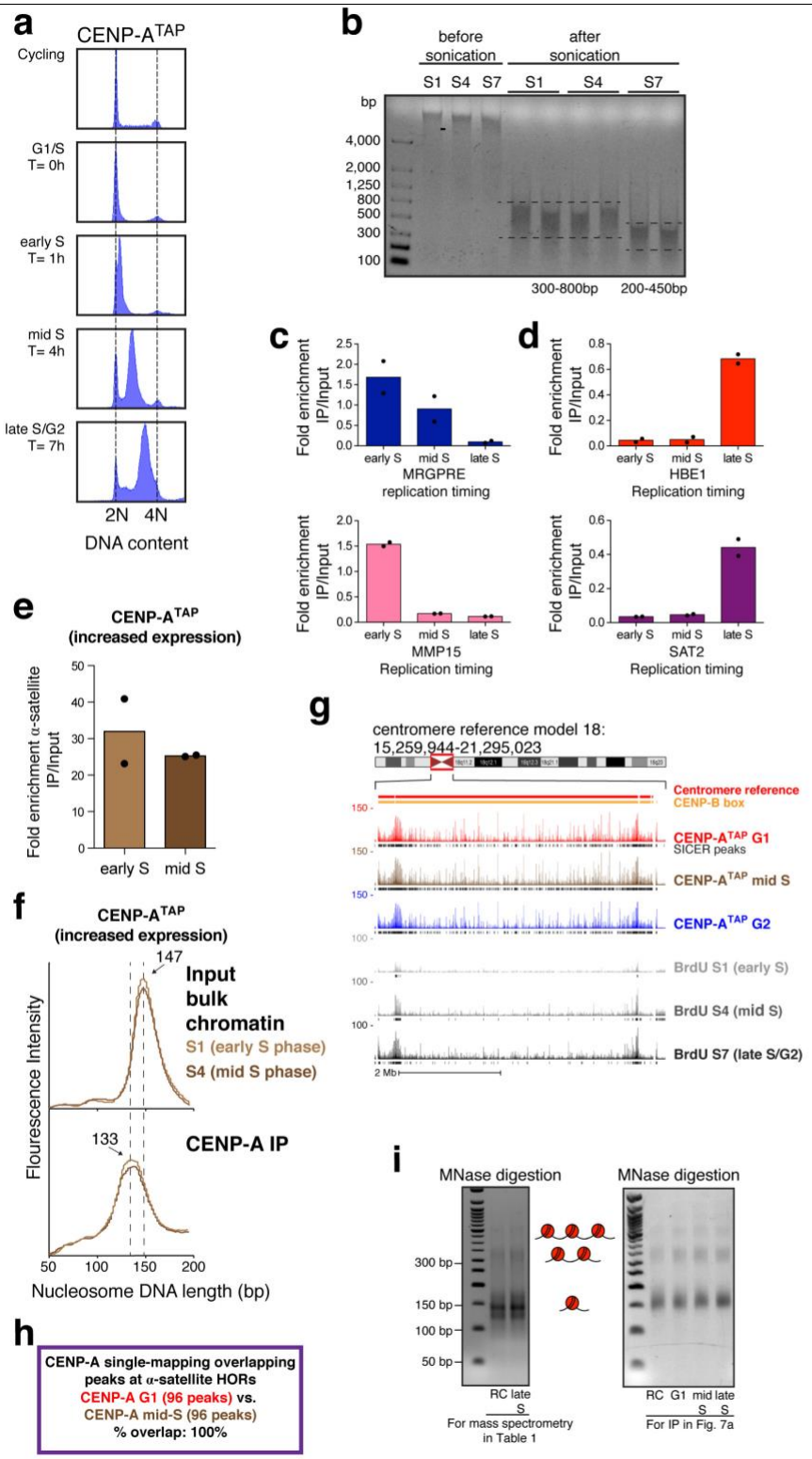

j MCM2-7 and CAF1 complexes

	Randomly cycling		late S/G2	
	spectra counts	peptide counts	spectra counts	peptide counts
MCM2	0	0	15	11
MCM3	19	10	26	15
MCM4	27	11	31	23
MCM5	20	9	30	17
MCM6	17	8	16	8
MCM7	71	22	79	32
CAF1p150	0	0	2	2
CAF1p48	37	8	19	12

k DNA replication related proteins

	Randomly cycling		late S/G2	
	spectra counts	peptide counts	spectra counts	peptide counts
RFC1	85	30	31	14
RFC2	38	14	29	13
RFC3	24	13	14	9
RFC4	41	17	27	16
RFC5	34	11	21	11
GINS2	0	0	4	3
GINS3	2	2	3	3
POLA1	7	5	9	9
POLD1	4	4	17	12
ORC1	24	19	15	13
ORC5	5	2	12	6
PCNA	6	5	3	3
CDC45	0	0	6	4

l Chromatin remodeling factors and nuclear chaperon

	Randomly cycling		late S/G2	
	spectra counts	peptide counts	spectra counts	peptide counts
HJURP	469	90	430	87
NPM1	415	45	282	43
RbAp46	29	13	19	11
NPM3	10	5	8	3
RSF1	306	79	73	39
FACTp80	430	79	181	59
FACTp140	1725	147	434	107
DAXX	12	7	0	0
NAP1L1	15	6	25	8
NAP1L4	4	3	5	3

m Histones

	Randomly cycling		late S/G2	
	spectra counts	peptide counts	spectra counts	peptide counts
H2A	1,924	96	810	81
H2B	520	31	205	25
H3.1	245	26	93	22
H4	737	48	396	66
H1	26	15	12	8

n centromere and kinetochore

	Randomly cycling		late S/G2	
	spectra counts	peptide counts	spectra counts	peptide counts
AURKB	8	7	16	12
Borealin	10	6	9	9
INCENP	12	10	14	13
KNL1	98	47	0	0
ZWINT	16	7	25	9
NDC80	5	3	48	26
NUF2	0	0	6	6
SPC24	0	0	19	7
SPC25	11	4	22	9
DSN1	47	18	47	19
MIS12	19	9	16	9
PMF1	20	11	19	11
NSL1	81	17	47	12
Mis18α	15	5	0	0
Mis18β	14	7	9	6
Mis18bp1	36	22	27	19

Supplementary Figure 5

Centromeres are late replicating with CENP-A remaining tethered locally by continued binding to the CCAN complex.

(**a**) FACS analysis of DNA content showing the synchronization efficiency of CENP-A$_{TAP}$ HeLa cell line across S phase. The experiment was repeated independently twice with similar results. (**b**) Genomic DNA of cells labeled for 1 hour with BrdU was sonicated prior to the BrdU immunoprecipitation and fragments of 200-800bp were obtained. The experiment was repeated independently twice with similar results. Unprocessed images of DNA gels can be found in Supplementary Fig. 6. (**c**) Quantitative real-time PCR for MRGPRE and MMP15 genes, previously reported to replicate early (ref$_9$ and ENCODE Repli-seq). (**d**) Quantitative real-time PCR for HBE1 and Sat2$_{10}$ genes, previously reported to replicate late (ref$_{11}$ and ENCODE Repli-seq). (**e**) Quantitative real-time PCR for α-satellite DNA. Data shown in c-e are from two biologically independent experiments. Source data for c-e can be found in Supplementary Table 4. (**f**) MNase digestion profile showing the nucleosomal DNA length distributions of bulk input mono-nucleosomes (upper panel) and purified CENP-A$_{TAP}$ following native ChIP at early S and mid S phase. The experiment was repeated twice independently with similar results. (**g**) CENP-A ChIP-seq raw mapping data spanning the whole of cen18 at G1, mid S phase and G2, and BrdU repli-seq at early S (S1), mid S (S4) and late S/G2 (S7). SICER peaks are denoted as black lines underneath the raw mapping data. The experiment was repeated twice independently with similar results. Centromere reference location, red. CENP-B boxes, orange. Scale bar, 2Mb. (**h**) Overlap degree between CENP-A G1 and mid-S at α-satellite HORs single copy variants. (**i**) Ethidium Bromide stained DNA agarose gel showing MNase digestion profile of bulk chromatin used for mass spectrometry identification of proteins associating with CENP-A$_{TAP}$ chromatin (left panel) and for CENP-A$_{TAP}$ co-immunoprecipitation experiment (right panel). Mass spectrometry was performed once and co-IP was performed twice with similar results. Unprocessed images of DNA gels can be found in Supplementary Fig. 6. (**j-n**) CENP-A$_{TAP}$ immunopurification followed by mass spectrometry identifies association with CENP-A chromatin of DNA replication related proteins (**j,k**), chromatin remodeling factors and nuclear chaperones (**l**), histones (**m**) and centromere and kinetochore proteins (**n**).

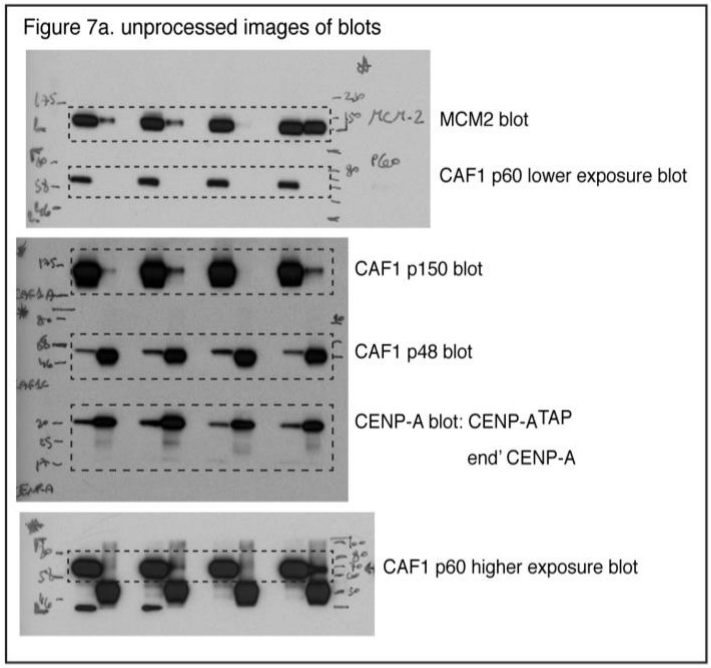

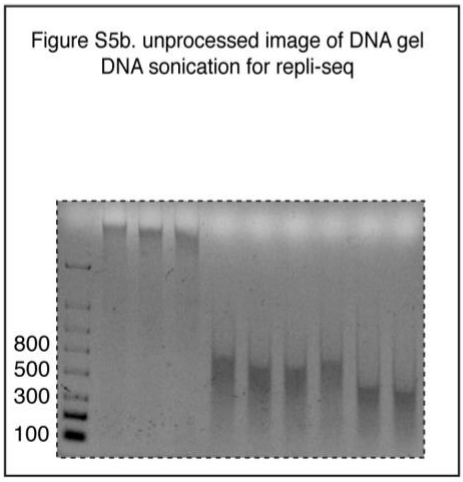

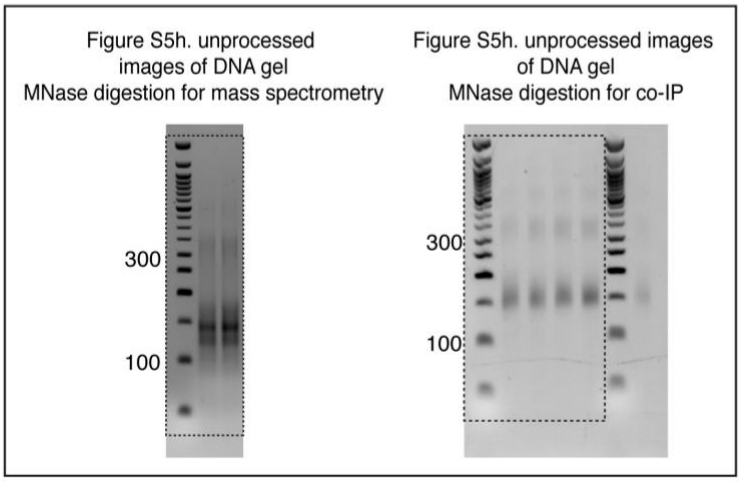

Supplementary Figure 6

Unprocessed film scans of all immunoblots and DNA gels with corresponding protein and DNA size markers.

Supplementary Video 1. Rapid CENP-C$_{AE/AE}$ depletion following IAA treatment. DLD1 CENP-C$_{AE/AE}$ [12] cells were treated with IAA and immediately filmed every 10 minutes. Green, CENP-C$_{AE/AE}$. Magenta, DNA labeled with Sir-DNA dye. Time (in minutes) is indicated in white. The experiment was repeated four times independently with similar results.

Supplementary Table 1. Read statistics for ChIP-seq and Repli-seq experiments. Total number of merged paired-end read (one read per merged two paired-ends) generated for each sample in dataset, the number (and percentage) of those that were >=100bp in length and the number (and percentage) of reads mapping to α-satellites. **Table A, B.** Read statistics for each sample in the CENP-A$_{+/LAP}$ dataset (A) and for the combined replicates in the CENP-A$_{+/LAP}$ dataset (D) in each condition. **Table C, D.** Read statistics for each sample in the CENP-A$_{TAP}$ dataset (C) and for the combined replicates in the CENP-A$_{TAP}$ dataset (D) in each condition. **Table E, F.** Read statistics for each sample in the BrdU Repli-seq dataset (E) and for the combined replicates in the BrdU Repli-seq dataset (F) in each condition.

Supplementary Table 2. Endogenous CENP-A sequence mapping onto α-satellite DNAs in human centromere reference models for each autosome and the X chromosome. Centromere reference models[3] were generated with methods as previously described[2]. Length estimates are expected to be averaged across arrays from homologous chromosomes. **Column 1:** chromosome information, **column 2:** chromosome start position, **column 3:** chromosome end position, **column 4:** length in bp of each reference model as represented in the human assembly[1, 3], **column 5:** Genbank accession, **columns 6:** Genomic locus, if applicable, **column 7, 8, 9:** number of reads for CENP-A$_{LAP}$ G1, replicate samples 1 and 2, and input, respectively, that aligned to the α-satellite reference model, **columns 10, 11, 12:** relative frequency of alignment to the α-satellite reference model is given for CENP-A$_{LAP}$ G1, replicate samples 1 and 2, and input, respectively. **Columns 13, 14:** fold-enrichment of CENP-A$_{LAP}$ G1, replicate samples 1 and 2 at the α-satellite reference model, relative to input. A summary of the reads and bases is given for those chromosomes that have several α-satellite reference models. Arrays that are identical between different chromosome locations are indicated as follows: *Sum of three near-identical arrays on chr1, 5, and 19; **Sum of two near-identical arrays on chr5, and 19; ***Sum of acrocentric near-identical arrays on chr13, 14, 21 and 22. Sequence coordinates refer to the human GRCh38 assembly.

Supplementary Table 3. Antibodies used in the study.

Supplementary Table 4. Statistical source data for graphical representations. The Statistical source data table provides the experimental data used to generate the graphical representations in the study.

References

1. Nechemia-Arbely, Y. *et al.* Human centromeric CENP-A chromatin is a homotypic, octameric nucleosome at all cell cycle points. *J Cell Biol* **216**, 607-621 (2017).

2. Miga, K.H. *et al.* Centromere reference models for human chromosomes X and Y satellite arrays. *Genome Res* **24**, 697-707 (2014).

3. Schneider, V.A. *et al.* Evaluation of GRCh38 and de novo haploid genome assemblies demonstrates the enduring quality of the reference assembly. *Genome Res* **27**, 849-864 (2017).

4. Ly, P. *et al.* Selective Y centromere inactivation triggers chromosome shattering in micronuclei and repair by non-homologous end joining. *Nat Cell Biol* **19**, 68-75 (2017).

5. Hasson, D. *et al.* The octamer is the major form of CENP-A nucleosomes at human centromeres. *Nat Struct Mol Biol* **20**, 687-695 (2013).

6. Hasson, D. *et al.* Formation of novel CENP-A domains on tandem repetitive DNA and across chromosome breakpoints on human chromosome 8q21 neocentromeres. *Chromosoma* **120**, 621-632 (2011).

7. Thakur, J. & Henikoff, S. Unexpected conformational variations of the human centromeric chromatin complex. *Genes Dev* **32**, 20-25 (2018).

8. Henikoff, J.G., Thakur, J., Kasinathan, S. & Henikoff, S. A unique chromatin complex occupies young alpha-satellite arrays of human centromeres. *Sci Adv* **1** (2015).

9. Ryba, T., Battaglia, D., Pope, B.D., Hiratani, I. & Gilbert, D.M. Genome-scale analysis of replication timing: from bench to bioinformatics. *Nat Protoc* **6**, 870-895 (2011).

10. Ohzeki, J. *et al.* Breaking the HAC Barrier: histone H3K9 acetyl/methyl balance regulates CENP-A assembly. *Embo J* **31**, 2391-2402 (2012).

11. Hassan, K.M., Norwood, T., Gimelli, G., Gartler, S.M. & Hansen, R.S. Satellite 2 methylation patterns in normal and ICF syndrome cells and association of hypomethylation with advanced replication. *Hum Genet* **109**, 452-462 (2001).

12. Hoffmann, S. *et al.* CENP-A Is Dispensable for Mitotic Centromere Function after Initial Centromere/Kinetochore Assembly. *Cell Rep* **17**, 2394-2404 (2016).

Table 1. Mass spectrometry of CENP-A individual nucleosomes reveal all the CCAN network components co-precipitated with CENP-A at late S/G2. CENP-A^{TAP} was immunoprecipitated from the chromatin fraction of randomly cycling cells or late S/G2 synchronized cells followed by mass spectrometry to identify the co-precipitated partners.

			Randomly cycling		Late S/G2	
			Spectra counts	Peptide counts	Spectra counts	Peptide counts
		CENP-A	107	22	70	21
		CENP-B	106	35	89	36
		CENP-V	11	7	6	5
CCAN	1	CENP-C	542	94	324	94
	2	CENP-L	68	19	37	16
	3	CENP-N	96	31	61	31
	4	CENP-H	49	17	28	11
	5	CENP-I	181	32	90	32
	6	CENP-K	206	32	93	28
	7	CENP-M	22	7	14	6
	8	CENP-O	21	8	14	9
	9	CENP-P	61	13	64	15
	10	CENP-Q	65	22	52	22
	11	CENP-U	111	28	52	22
	12	CENP-R	54	13	24	8
	13	CENP-T	87	22	35	20
	14	CENP-W	0	0	5	3
	15	CENP-S	25	6	11	4
	16	CENP-X	29	6	15	3

Supplementary Table S1. Read statistics for ChIP-seq and Repli-seq experiments. Total number of merged paired-end read (one read per merged two paired-ends) generated for each sample in dataset, the number (and percentage) of those that were >=100bp in length and the number (and percentage) of reads mapping to α-satellites. **Table A, B.** Read statistics for each sample in the CENP-A$^{+/LAP}$ dataset (A) and for the combined replicates in the CENP-A$^{+/LAP}$ dataset (D) in each condition. **Table C, D.** Read statistics for each sample in the CENP-A^{TAP} dataset (C) and for the combined replicates in the CENP-A^{TAP} dataset (D) in each condition. **Table E, F.** Read statistics for each sample in the BrdU Repli-seq dataset (E) and for the combined replicates in the BrdU Repli-seq dataset (F) in each condition.

Table A. ChIP-seq replicates statistics for CENP-A$^{+/LAP}$ chromatin

Experiment	Replicate No	Total number of merged paired-end reads (100bp x 2)	Total (%) number of merged reads >=100bp	No (%) of merged reads mapping to α-satellites
CENP-A^{LAP} G1	1	37,088,538	30,232,099 (81.5%)	27,671,623 (74.6%)
	2	40,641,911	33,438,763 (82.3%)	30,342,295 (74.6%)
CENP-A^{LAP} G2	1	39,939,734	32,202,885 (80.6%)	24,209,577 (60.6%)
	2	32,689,317	25,933,735 (79.3%)	19,566,369 (59.9%)
CENP-A^{LAP} G1 Input	1	31,874,876	28,835,317 (90.5%)	952,554 (2.98%)
CENP-A^{LAP} G2 Input	1	74,252,732	68,409,198 (92.1%)	2,200,921 (2.96%)

Table B. ChIP-seq combined replicate statistics for CENP-A$^{+/LAP}$ chromatin

Experiment	Total number of merged paired-end reads (100bp x 2)	Total (%) number of merged reads >=100bp	No (%) of merged reads mapping to α-satellites
CENP-A^{LAP} G1	77,730,449	63,670,862 (81.9%)	58,013,918 (74.6%)
CENP-A^{LAP} G2	72,629,051	58,136,620 (79.9%)	43,775,946 (60.2%)

Table C. ChIP-seq replicates statistics for CENP-A^{TAP} chromatin				
Experiment	**Replicate No**	**Total number of merged paired-end reads (100bp x 2)**	**Total (%) number of merged reads >=100bp**	**No (%) of merged reads mapping to α-satellites**
CENP-A^{TAP} RC	1	9,436,346	8,464,391 (89.7%)	4,588,228 (48.6%)
	2	69,039,423	54,952,932 (79.6%)	31,053,433 (45%)
CENP-A^{TAP} G1	1	68,776,382	54,522,683 (79.3%)	28,023,214 (40.7%)
	2	51,746,426	40,328,176 (77.9%)	21,534,570 (41.6%)
CENP-A^{TAP} mid S	1	65,077,481	50,476,007 (77.6%)	33,879,664 (52.1%)
	2	62,298,174	48,772,959 (78.3%)	31,783,490 (51.0%)
CENP-A^{TAP} G2	1	49,206,313	40,088,665 (81.5%)	25,204,739 (51.2%)
	2	60,985,667	48,764,504 (80.0%)	33,414,704 (54.8%)
H3.1^{TAP} RC	1	31,819,170	27,823,087 (87.4%)	668,075 (2.1%)
	2	42,069,089	36,187,314 (86.0%)	911,027 (2.2%)
CENP-A^{TAP} RC Input	1	61,557,119	61,612,349 (84.5%)	1,374,644 (2.2%)
CENP-A^{TAP} G1 Input	1	58,262,947	48,941,720 (84%)	1,691,920 (2.9%)
CENP-A^{TAP} G2 Input	1	50,117,787	41,826,112 (83.5%)	1,674,557 (3.34%)

Table D. ChIP-seq combined replicate statistics for CENP-A^{TAP} chromatin			
Experiment	**Total number of merged paired-end reads (100bp x 2)**	**Total (%) number of merged reads >=100bp**	**No (%) of merged reads mapping to α-satellites**
CENP-A^{TAP} RC	78,475,769	63,417,323 (80.8%)	35,641,661 (46.8%)
CENP-A^{TAP} G1	120,522,808	94,850,859 (78.7%)	49,557,784 (41.2%)
CENP-A^{TAP} mid S	127,375,655	99,248,966 (77.9%)	65,663,154 (51.5%)
CENP-A^{TAP} G2	110,191,980	88,853,169 (80.6%)	58,619,443 (53%)
H3.1^{TAP} RC	73,888,259	64,010,401 (86.6%)	1,579,102 (2.15%)

Table E. Repli-seq replicates statistics for BrdU labeled DNA				
Experiment	**Replicate No**	**Total number of merged paired-end reads (100bp x 2)**	**Total (%) number of merged reads >=100bp**	**No (%) of merged reads mapping to α-satellites**
BrdU S1 Early S phase	1	48,838,225	42,840,706 (87.7%)	144,337 (0.29%)
	2	938,746	730,915 (77.8%)	2,082 (0.22%)
BrdU S4 Mid S phase	1	46,828,553	40,991,823 (87.5%)	371,793 (0.79%)
	2	34,480,560	31,507,686 (91.4%)	254,159 (0.73%)
BrdU S7 Late S phase	1	40,899,839	35,827,676 (87.6%)	1,657,902 (4.05%)
	2	41750,126	35,667,382 (85.4%)	1,682,353 (4.03%)
BrdU S1 Input	1	22,887,332	21,177,083 (92.5%)	1,185,850 (5.2%)
BrdU S4 Input	1	25,806,345	23,810,449 (92.2%)	1,146,797 (4.4%)
BrdU S7 Input	1	25,004,047	23,205,784 (92.8%)	1,322,554 (5.3%)

Table F. Repli-seq combined replicate statistics for BrdU labeled DNA			
Experiment	**Total number of merged paired-end reads (100bp x 2)**	**Total (%) number of merged reads >=100bp**	**No (%) of merged reads mapping to α-satellites**
BrdU S1 Early S phase	49,776,971	43,571,621 (82.8%)	146,419 (0.25%)
BrdU S4 Mid S phase	81,309,113	72,499,509 (89.4%)	625,952 (0.76%)
BrdU S7 Late S phase	82,649,965	71,495,058 (86.5%)	3,340,255 (4.04%)

Table S2. Endogenous CENP-A sequence mapping onto α-satellite DNAs in human centromere reference models for each autosome and the X chromosome. Centromere reference models are from Miga et al. ([46], unpublished), generated with methods as previously described [45]. Length estimates are expected to be averaged across arrays from homologous chromosomes. **Column 1:** chromosome information, **column 2:** chromosome start position, **column 3:** chromosome end position, **column 4:** length in bp of each reference model as represented in the human assembly [46, 8], **column 5:** Genbank accession, **columns 6:** Genomic locus, if applicable, **column 7, 8, 9:** number of reads for CENP-A^{LAP} G1, replicate samples 1 and 2, and input, respectively, that aligned to the α-satellite reference model, **columns 10, 11, 12:** relative frequency of alignment to the α-satellite reference model is given for CENP-A^{LAP} G1, replicate samples 1 and 2, and input, respectively. **Columns 13, 14:** fold-enrichment of CENP-A^{LAP} G1, replicate samples 1 and 2 at the α-satellite reference model, relative to input. A summary of the reads and bases is given for those chromosomes that have several α-satellite reference models. Arrays that are identical between different chromosome locations are indicated as follows: *Sum of three near-identical arrays on chr1, 5, and 19; **Sum of two near-identical arrays on chr5, and 19; ***Sum of acrocentric near-identical arrays on chr13, 14, 21 and 22. Sequence coordinates refer to the human GRCh38 assembly.

hg38 chromo-some number	chromosome coordinates Start	chromosome coordinates End	Length (bp)	GenBank Accession number	Locus	CENP-A G1-1 Read count	CENP-A G1-2 Read count	Input Read count	CENP-A G1-1 Relative Frequency	CENP-A G1-2 Relative Frequency	Input Relative Frequency	CENP-A G1-1 Enrichment	CENP-A G1-2 Enrichment
chr1	122,026,459	122,224,535	198,076	GJ211836.1	N/A	465	400	354	1.29E-05	1.05E-05	1.11E-05	1.16	0.94
chr1	122,224,635	122,503,147	278,512	GJ211837.1	D1Z5	6,636	6,492	2,363	1.84E-04	1.70E-04	7.43E-05	2.48	2.29
chr1*	122,503,247	124,785,432	2,282,185	GJ212202.1	D1Z7/ D5Z2/ D19Z3	3,884,766	4,104,057	153,199	1.08E-01	1.08E-01	4.82E-03	**22.41**	**22.35**
chr1	124,785,532	124,849,129	63,597	GJ211855.1	N/A	1,154	1,189	797	3.21E-05	3.12E-05	2.51E-05	1.28	1.24
chr1	124,849,229	124,932,724	83,495	GJ211857.1	N/A	4,408	4,565	965	1.22E-04	1.20E-04	3.03E-05	4.04	3.95
Sum chr1			**2,905,865**			**3,897,429**	**4,116,703**	**157,678**	**1.08E-01**	**1.08E-01**	**4.96E-03**	**21.84**	**21.78**
chr2	**92,188,145**	**94,090,557**	**1,902,412**	**GJ211860.1**	**D2Z1**	**772,858**	**773,709**	**13,622**	**2.15E-02**	**2.03E-02**	**4.28E-04**	**50.14**	**47.39**
chr3	90,772,458	91,233,586	461,128	GJ211866.1	N/A	3,287	2,626	3,396	9.13E-05	6.89E-05	1.07E-04	0.86	0.65
chr3	91,233,686	91,247,622	13,936	GJ211867.1	N/A	90	93	146	2.50E-06	2.44E-06	4.59E-06	0.54	0.53
chr3	91,553,419	93,655,574	2,102,155	GJ211871.1	D3Z1	726,106	743,093	59,085	2.02E-02	1.95E-02	1.86E-03	**10.86**	**10.49**
Sum chr3			**2,577,219**			**729,483**	**745,812**	**62,627**	**2.03E-02**	**1.96E-02**	**1.97E-03**	**10.29**	**9.94**
chr4	**49,712,061**	**51,743,951**	**2,031,890**	**GJ211881.1**	**D4Z1**	**802,017**	**880,598**	**25,601**	**2.23E-02**	**2.31E-02**	**8.05E-04**	**27.69**	**28.70**
chr5	46,485,900	46,569,062	83,162	GJ211882.1	N/A	1,138	1,262	727	3.16E-05	3.31E-05	2.29E-05	1.38	1.45
chr5	46,569,162	46,796,725	227,563	GJ211883.1	N/A	1,055	1,064	632	2.93E-05	2.79E-05	1.99E-05	1.48	1.40
chr5	46,796,825	47,061,288	264,463	GJ211884.1	N/A	2,175	2,406	1,712	6.04E-05	6.31E-05	5.38E-05	1.12	1.17
chr5	47,106,994	47,153,339	46,345	GJ211886.1	N/A	1,180	1,321	864	3.28E-05	3.47E-05	2.72E-05	1.21	1.28
chr5	47,153,439	47,296,069	142,630	GJ211887.1	N/A	1,589	1,669	361	4.42E-05	4.38E-05	1.14E-05	3.89	3.86

chr5*	47,309,184	49,591,369	2,282,185	GJ212203.1	D1Z7/ D5Z2/ D19Z3	3,884,766	4,104,057	153,199	1.08E-01	1.08E-01	4.82E-03	**22.41**	**22.35**
chr5**	49,667,531	49,721,203	53,672	GJ211904.2	N/A	421	377	464	1.17E-05	9.89E-06	1.46E-05	0.80	0.68
chr5	49,721,303	50,059,807	338,504	GJ211906.2	N/A	1,094	1,196	1,456	3.04E-05	3.14E-05	4.58E-05	0.66	0.69
Sum chr5			**3,438,524**			**3,893,418**	**4,113,352**	**159,415**	**1.08E-01**	**1.08E-01**	**5.01E-03**	**21.58**	**21.53**
chr6	**58,553,888**	**59,829,934**	**1,276,046**	**GJ211907.1**	**D6Z1**	**1,240,000**	**1,360,728**	**41,164**	**3.45E-02**	**3.57E-02**	**1.29E-03**	**26.62**	**27.58**
chr7	58,169,653	60,828,234	2,658,581	GJ211908.1	D7Z1	987,890	1,080,834	25,905	2.75E-02	2.84E-02	8.15E-04	**33.70**	**34.81**
chr7	61,377,788	61,528,020	150,232	GJ212194.1	D7Z2	1,818	1,897	890	5.05E-05	4.98E-05	2.80E-05	1.81	1.78
Sum chr7			**2,808,813**			**989,708**	**1,082,731**	**26,795**	**2.75E-02**	**2.84E-02**	**8.43E-04**	**32.64**	**33.71**
chr8	**44,033,744**	**45,877,265**	**1,843,521**	**GJ211909.1**	**D8Z2**	**962,237**	**1,055,322**	**21,112**	**2.67E-02**	**2.77E-02**	**6.64E-04**	**40.28**	**41.70**
chr9	**43,389,635**	**45,518,558**	**2,128,923**	**GJ211929.1**	**D9Z4**	**726,448**	**801,194**	**16,178**	**2.02E-02**	**2.10E-02**	**5.09E-04**	**39.68**	**41.32**
chr10	39,686,682	39,935,900	249,218	GJ211930.1	N/A	215,957	211,519	859	6.00E-03	5.55E-03	2.70E-05	**222.18**	**205.43**
chr10	39,936,000	41,497,440	1,561,440	GJ211932.1	D10Z1	503,166	508,384	14,260	1.40E-02	1.33E-02	4.48E-04	31.18	29.74
chr10	41,497,540	41,545,720	48,180	GJ211933.1	N/A	18,519	16,696	1,314	5.15E-04	4.38E-04	4.13E-05	12.46	10.60
chr10	41,545,820	41,593,521	47,701	GJ211936.1	N/A	4,002	3,829	1,465	1.11E-04	1.00E-04	4.61E-05	2.41	2.18
Sum chr10			**1,906,539**			**741,644**	**740,428**	**17,898**	**2.06E-02**	**1.94E-02**	**5.63E-04**	**36.62**	**34.51**
chr11	51,078,348	51,090,317	11,969	GJ211938.1	N/A	63	23	29	1.75E-06	6.03E-07	9.12E-07	1.92	0.66
chr11	51,090,417	54,342,399	3,251,982	GJ211943.1	D11Z1	811,562	827,321	35,762	2.26E-02	2.17E-02	1.12E-03	**20.06**	**19.30**
chr11	54,342,499	54,425,074	82,575	GJ211948.1	N/A	74,089	75,567	2,855	2.06E-03	1.98E-03	8.98E-05	**22.93**	**22.08**
Sum chr11			**3,346,526**			**885,714**	**902,911**	**38,646**	**2.46E-02**	**2.37E-02**	**1.22E-03**	**20.25**	**19.49**
chr12	34,769,407	34,816,611	47,204	GJ211949.1	N/A	773	477	274	2.15E-05	1.25E-05	8.62E-06	2.49	1.45
chr12	34,835,295	37,185,252	2,349,957	GJ211954.1	D12Z3	1,559,732	1,576,847	59,791	4.33E-02	4.14E-02	1.88E-03	**23.05**	**22.00**
Sum chr12			**2,397,161**			**1,560,505**	**1,577,324**	**60,065**	**4.34E-02**	**4.14E-02**	**1.89E-03**	**22.96**	**21.91**
chr13***	16,000,000	16,022,537	22,537	GJ211955.2	N/A	417	417	429	1.16E-05	1.09E-05	1.35E-05	0.86	0.81
chr13***	16,022,637	16,110,659	88,022	GJ211961.2	N/A	556	529	587	1.54E-05	1.39E-05	1.85E-05	0.84	0.75
chr13***	16,110,759	16,164,892	54,133	GJ211962.2	N/A	2,684	2,706	3,491	7.46E-05	7.10E-05	1.10E-04	0.68	0.65
chr13***	16,164,992	16,228,527	63,535	GJ211963.2	N/A	1,392	1,369	1,549	3.87E-05	3.59E-05	4.87E-05	0.79	0.74
chr13***	16,228,627	16,249,297	20,670	GJ211965.2	N/A	1,621	1,627	1,914	4.50E-05	4.27E-05	6.02E-05	0.75	0.71
chr13***	16,249,397	16,256,067	6,670	GJ211967.2	N/A	2,773	2,699	1,877	7.71E-05	7.08E-05	5.90E-05	1.31	1.20

chr13***	16,256,167	16,259,412	3,245	GJ211968.2	N/A	64	61	53	1.78E-06	1.60E-06	1.67E-06	1.07	0.96
chr13***	16,259,512	16,282,073	22,561	GJ211969.2	N/A	290	294	274	8.06E-06	7.71E-06	8.62E-06	0.94	0.90
chr13***	16,282,173	17,416,384	1,134,211	GJ211972.2	N/A	2,485,354	2,490,600	50,193	6.91E-02	6.53E-02	1.58E-03	**43.76**	**41.40**
chr13***	17,416,484	17,416,824	340	GJ212205.1	N/A	12	15	1	3.33E-07	3.93E-07	3.14E-08	**10.60**	**12.51**
chr13***	17,416,924	17,417,264	340	GJ212206.1	N/A	29	34	1	8.06E-07	8.92E-07	3.14E-08	**25.63**	**28.37**
chr13***	17,417,364	17,418,562	1,198	GJ211986.2	N/A	576	563	432	1.60E-05	1.48E-05	1.36E-05	1.18	1.09
chr13***	17,418,662	18,051,248	632,586	GJ211991.2	D13Z1/ D21Z1 alphaRI, L1.26	1,535,634	1,543,548	24,960	4.27E-02	4.05E-02	7.85E-04	**54.37**	**51.59**
Sum chr13			**2,050,048**			**4,031,402**	**4,044,462**	**85,761**	**1.12E-01**	**1.06E-01**	**2.70E-03**	**41.54**	**39.34**
chr14***	16,000,000	16,022,537	22,537	GJ211992.2	N/A	417	417	429	1.16E-05	1.09E-05	1.35E-05	0.86	0.81
chr14***	16,140,627	16,228,649	88,022	GJ211998.2	N/A	556	529	587	1.54E-05	1.39E-05	1.85E-05	0.84	0.75
chr14***	16,228,749	16,282,882	54,133	GJ211999.2	N/A	2,684	2,706	3,491	7.46E-05	7.10E-05	1.10E-04	0.68	0.65
chr14***	16,282,982	16,346,517	63,535	GJ212000.2	N/A	1,392	1,369	1,549	3.87E-05	3.59E-05	4.87E-05	0.79	0.74
chr14***	16,346,617	16,367,287	20,670	GJ212002.2	N/A	1,621	1,627	1,914	4.50E-05	4.27E-05	6.02E-05	0.75	0.71
chr14***	16,367,387	16,374,057	6,670	GJ212004.2	N/A	2,773	2,699	1,877	7.71E-05	7.08E-05	5.90E-05	1.31	1.20
chr14***	16,374,157	16,377,402	3,245	GJ212005.2	N/A	64	61	53	1.78E-06	1.60E-06	1.67E-06	1.07	0.96
chr14***	16,377,502	16,400,063	22,561	GJ212006.2	N/A	290	294	274	8.06E-06	7.71E-06	8.62E-06	0.94	0.90
chr14***	16,404,448	17,538,659	1,134,211	GJ212009.2	N/A	2,485,354	2,490,600	50,193	6.91E-02	6.53E-02	1.58E-03	**43.76**	**41.40**
chr14***	17,538,759	17,539,099	340	GJ212210.1	N/A	12	15	1	3.33E-07	3.93E-07	3.14E-08	**10.60**	**12.51**
chr14***	17,539,199	17,539,539	340	GJ212211.1	N/A	29	34	1	8.06E-07	8.92E-07	3.14E-08	**25.63**	**28.37**
chr14***	17,539,639	17,540,837	1,198	GJ212023.2	N/A	576	563	432	1.60E-05	1.48E-05	1.36E-05	1.18	1.09
chr14***	17,540,937	18,173,523	632,586	GJ212028.2	N/A	1,535,634	1,543,548	24,960	4.27E-02	4.05E-02	7.85E-04	**54.37**	**51.59**
Sum chr14			**2,050,048**			**4,031,402**	**4,044,462**	**85,761**	**1.12E-01**	**1.06E-01**	**2.70E-03**	**41.54**	**39.34**
chr15	17,083,673	17,498,951	415,278	GJ212036.1	N/A	1,740	1,718	1,281	4.83E-05	4.51E-05	4.03E-05	1.20	1.12
chr15	17,499,051	18,355,008	855,957	GJ212042.1	N/A	9,617	9,910	4,554	2.67E-04	2.60E-04	1.43E-04	1.87	1.82
chr15	18,355,108	19,725,254	1,370,146	GJ212045.1	D15Z3	1,195,175	1,187,663	14,547	3.32E-02	3.12E-02	4.57E-04	**72.61**	**68.11**
Sum chr15			**2,641,381**			**1,206,532**	**1,199,291**	**20,382**	**3.35E-02**	**3.15E-02**	**6.41E-04**	**52.31**	**49.09**
chr16	36,311,158	36,334,460	23,302	GJ212046.1	N/A	419	387	147	1.16E-05	1.02E-05	4.62E-06	2.52	2.20

chr16	36,337,666	38,265,669	1,928,003	GJ212051.1	D16Z2	857,505	872,514	19,641	2.38E-02	2.29E-02	6.18E-04	**38.58**	**37.06**
Sum chr16			**1,951,305**			**857,924**	**872,901**	**19,788**	**2.38E-02**	**2.29E-02**	**6.22E-04**	**38.32**	**36.80**
chr17	22,813,679	23,194,918	381,239	GJ212053.1	D17Z1B	48,160	47,722	2,792	1.34E-03	1.25E-03	8.78E-05	**15.24**	**14.26**
chr17	23,195,018	26,566,633	3,371,615	GJ212054.1	D17Z1	358,116	338,203	11,231	9.95E-03	8.87E-03	3.53E-04	**28.18**	**25.12**
chr17	26,566,733	26,616,164	49,431	GJ212055.1	N/A	87,241	90,634	2,765	2.42E-03	2.38E-03	8.69E-05	**27.88**	**27.35**
Sum chr17			**3,802,285**			**493,517**	**476,559**	**16,788**	**1.37E-02**	**1.25E-02**	**5.28E-04**	**25.98**	**23.68**
chr18	15,460,899	15,780,377	319,478	GJ212060.1	N/A	16,312	15,458	2,974	4.53E-04	4.05E-04	9.35E-05	4.85	4.34
chr18	15,797,855	20,561,439	4,763,584	GJ212062.1	D18Z1	530,474	534,958	16,477	1.47E-02	1.40E-02	5.18E-04	**28.45**	**27.09**
chr18	20,603,247	20,696,289	93,042	GJ212066.1	D18Z2	2,198	2,120	737	6.11E-05	5.56E-05	2.32E-05	2.64	2.40
chr18	20,696,389	20,736,025	39,636	GJ212067.1	N/A	503	386	127	1.40E-05	1.01E-05	3.99E-06	3.50	2.54
chr18	20,736,125	20,813,083	76,958	GJ212069.1	N/A	812	650	170	2.26E-05	1.71E-05	5.35E-06	4.22	3.19
chr18	20,839,797	20,861,206	21,409	GJ212071.1	N/A	120	92	32	3.33E-06	2.41E-06	1.01E-06	3.31	2.40
Sum chr18			**5,314,107**			**550,419**	**553,664**	**20,517**	**1.53E-02**	**1.45E-02**	**6.45E-04**	**23.71**	**22.51**
chr19**	24,498,980	24,552,652	53,672	GJ212072.2	N/A	421	377	464	1.17E-05	9.89E-06	1.46E-05	0.80	0.68
chr19	24,552,752	24,891,256	338,504	GJ212077.2	N/A	1,176	1,165	1,617	3.27E-05	3.06E-05	5.08E-05	0.64	0.60
chr19*	24,908,689	27,190,874	2,282,185	GJ212201.1	D1Z7/ D5Z2/ D19Z3	3,884,766	4,104,057	153,199	1.08E-01	1.08E-01	4.82E-03	**22.41**	**22.35**
Sum chr19			**2,674,361**			**3,886,363**	**4,105,599**	**155,280**	**1.08E-01**	**1.08E-01**	**4.88E-03**	**22.12**	**22.06**
chr20	26,436,232	26,586,955	150,723	GJ212091.1	N/A	8,724	6,977	2,142	2.42E-04	1.83E-04	6.73E-05	3.60	2.72
chr20	26,608,145	28,494,539	1,886,394	GJ212093.1	D20Z2	578,724	588,963	11,545	1.61E-02	1.54E-02	3.63E-04	**44.30**	**42.56**
chr20	28,508,997	28,556,953	47,956	GJ212095.1	N/A	3,688	3,180	2,219	1.02E-04	8.34E-05	6.98E-05	1.47	1.20
chr20	28,648,108	28,728,874	80,766	GJ212105.1	N/A	279	276	378	7.75E-06	7.24E-06	1.19E-05	0.65	0.61
chr20	29,125,793	29,204,668	78,875	GJ212107.1	N/A	174	136	204	4.83E-06	3.57E-06	6.41E-06	0.75	0.56
chr20	29,917,404	30,038,348	120,944	GJ212117.1	N/A	379	246	297	1.05E-05	6.45E-06	9.34E-06	1.13	0.69
Sum chr20			**2,365,658**			**591,968**	**599,778**	**16,785**	**1.64E-02**	**1.57E-02**	**5.28E-04**	**31.17**	**29.81**
chr21***	10,864,560	10,887,097	22,537	GJ212118.2	N/A	417	417	429	1.16E-05	1.09E-05	1.35E-05	0.86	0.81
chr21***	10,887,197	10,975,219	88,022	GJ212124.2	N/A	556	529	587	1.54E-05	1.39E-05	1.85E-05	0.84	0.75
chr21***	10,975,319	11,029,452	54,133	GJ212125.2	N/A	2,684	2,706	3,491	7.46E-05	7.10E-05	1.10E-04	0.68	0.65
chr21***	11,029,552	11,093,087	63,535	GJ212126.2	N/A	1,392	1,369	1,549	3.87E-05	3.59E-05	4.87E-05	0.79	0.74

chr21***	11,093,187	11,113,857	20,670	GJ212128.2	N/A	1,621	1,627	1,914	4.50E-05	4.27E-05	6.02E-05	0.75	0.71
chr21***	11,113,957	11,120,627	6,670	GJ212130.2	N/A	2,773	2,699	1,877	7.71E-05	7.08E-05	5.90E-05	1.31	1.20
chr21***	11,120,727	11,123,972	3,245	GJ212131.2	N/A	64	61	53	1.78E-06	1.60E-06	1.67E-06	1.07	0.96
chr21***	11,124,072	11,146,633	22,561	GJ212132.2	N/A	290	294	274	8.06E-06	7.71E-06	8.62E-06	0.94	0.90
chr21***	11,146,733	12,280,944	1,134,211	GJ212135.2	N/A	2,485,354	2,490,600	50,193	6.91E-02	6.53E-02	1.58E-03	**43.76**	**41.40**
chr21***	12,281,044	12,281,384	340	GJ212204.1	N/A	12	15	1	3.33E-07	3.93E-07	3.14E-08	**10.60**	**12.51**
chr21***	12,281,484	12,281,824	340	GJ212207.1	N/A	29	34	1	8.06E-07	8.92E-07	3.14E-08	**25.63**	**28.37**
chr21***	12,281,924	12,283,122	1,198	GJ212149.2	N/A	576	563	432	1.60E-05	1.48E-05	1.36E-05	1.18	1.09
chr21***	12,283,222	12,915,808	632,586	GJ212154.2	D13Z1/ D21Z1 alphaRI, L1.26	1,535,634	1,543,548	24,960	4.27E-02	4.05E-02	7.85E-04	**54.37**	**51.59**
Sum chr21			**2,050,048**			**4,031,402**	**4,044,462**	**85,761**	**1.12E-01**	**1.06E-01**	**2.70E-03**	**41.54**	**39.34**
chr22***	12,954,788	12,977,325	22,537	GJ212155.2	N/A	417	417	429	1.16E-05	1.09E-05	1.35E-05	0.86	0.81
chr22***	13,021,422	13,109,444	88,022	GJ212161.2	N/A	556	529	587	1.54E-05	1.39E-05	1.85E-05	0.84	0.75
chr22***	13,109,544	13,163,677	54,133	GJ212162.2	N/A	2,684	2,706	3,491	7.46E-05	7.10E-05	1.10E-04	0.68	0.65
chr22***	13,163,777	13,227,312	63,535	GJ212163.2	N/A	1,392	1,369	1,549	3.87E-05	3.59E-05	4.87E-05	0.79	0.74
chr22***	13,227,412	13,248,082	20,670	GJ212165.2	N/A	1,621	1,627	1,914	4.50E-05	4.27E-05	6.02E-05	0.75	0.71
chr22***	13,248,182	13,254,852	6,670	GJ212167.2	N/A	2,773	2,699	1,877	7.71E-05	7.08E-05	5.90E-05	1.31	1.20
chr22***	13,254,952	13,258,197	3,245	GJ212168.2	N/A	64	61	53	1.78E-06	1.60E-06	1.67E-06	1.07	0.96
chr22***	13,258,297	13,280,858	22,561	GJ212169.2	N/A	290	294	274	8.06E-06	7.71E-06	8.62E-06	0.94	0.90
chr22***	13,285,243	14,419,454	1,134,211	GJ212172.2	N/A	2,485,354	2,490,600	50,193	6.91E-02	6.53E-02	1.58E-03	**43.76**	**41.40**
chr22***	14,419,554	14,419,894	340	GJ212208.1	N/A	12	15	1	3.33E-07	3.93E-07	3.14E-08	**10.60**	**12.51**
chr22***	14,419,994	14,420,334	340	GJ212209.1	N/A	29	34	1	8.06E-07	8.92E-07	3.14E-08	**25.63**	**28.37**
chr22***	14,420,434	14,421,632	1,198	GJ212186.2	N/A	576	563	432	1.60E-05	1.48E-05	1.36E-05	1.18	1.09
chr22***	14,421,732	15,054,318	632,586	GJ212191.2	N/A	1,535,634	1,543,548	24,960	4.27E-02	4.05E-02	7.85E-04	**54.37**	**51.59**
Sum chr22			**2,050,048**			**4,031,402**	**4,044,462**	**85,761**	**1.12E-01**	**1.06E-01**	**2.70E-03**	**41.54**	**39.34**
chrX	**58,605,579**	**62,412,542**	**3,806,963**	**GJ212192.1**	**DXZ1**	**725,621**	**794,981**	**17,185**	**2.02E-02**	**2.09E-02**	**5.40E-04**	**37.32**	**38.59**

Primary antibodies					
Antibody	**Species**	**Assay and dilution**	**Source**	**Catalogue**	**Validation**
BrdU	Mouse	Repli-seq	Becton-Dickinson Biosciences	CAT # 555627	used for Repli-seq previously (Hansen et al., 2010)
GFP	Mouse	CENP-A^{LAP} ChIP-seq	MSKCC antibody core facility	clone 19C8 and clone 19F7	validated previously by us and others
rabbit IgG	rabbit	CENP-A^{TAP} ChIP-seq	Sigma-Aldrich	CAT # I5006	validated previously by us (Foltz et al., 2006) and others
CENP-A	rabbit	Immunoblot 1:1,000	Cell Signaling Technology	CAT # 2186	validated in Fig. 6o, also previously used by us and others
CENP-A	mouse	ChIP	Abcam	CAT # Ab13939	used for ChIP previously (Hasson et al., 2013)
CAF1p150	rabbit	Immunoblot 1:500	Santa Cruz	CAT # sc-10772	validated in Fig. 6o; also see manufacturer's data sheet
CAF1p60	rabbit	Immunoblot 1:1,000	Bethyl Laboratories	CAT # A301-085A	validated in Fig. 6o; also see manufacturer's data sheet
CAF1p48	rabbit	Immunoblot 1:1,000	Bethyl Laboratories	CAT # A301-206A	validated in Fig. 6o; also see manufacturer's data sheet
MCM2	rabbit	Immunoblot 1:1,000	Abcam	CAT # Ab4461	validated in Fig. 6o; also see manufacturer's data sheet
CENP-B	rabbit	Immunofluorescence 1:1,000	Abcam	CAT # 25734	validated in Fig. S1d and previously by us and others
GFP	Mouse	Immunofluorescence 1:500	Roche	CAT # 11814460001	validated in Fig. S1c and previously by us and others
anti-centromere antibodies (ACA)	human	Immunofluorescence 1:500	Antibodies Inc	CAT # 15-234-0001	validated in Fig. S1c and previously by us and others
Secondary antibodies					
Antibody	**Species**	**Dilution**	**Source**	**Catalogue number**	
Sheep anti-mouse HRP	sheep	Immunoblot 1:4,000	GE Healthcare	NA931V	
donkey anti-rabbit HRP	donkey	Immunoblot 1:4,000	GE Healthcare	NA934V	
donkey anti-human TR	donkey	Immunofluorescence 1:300	Jackson Laboratories	CAT # 709-075-149	
donkey anti-mouse FITC	donkey	Immunofluorescence 1:250	Jackson Laboratories	CAT # 715-095-151	
FITC-rabbit IgG	rabbit	Immunofluorescence 1:200	Jackson Laboratories	CAT # 011-090-003	